PCCP

ROYAL SOCIETY OF CHEMISTRY

PAPER

View Article Online
View Journal | View Issue

Check for updates

Cite this: *Phys. Chem. Chem. Phys.*, 2022, **24**, 2454

The molecular structure and curious motions in 1,1-difluorosilacyclopent-3-ene and silacyclopent-3-ene as determined by microwave spectroscopy and quantum chemical calculations†

Thomas M. C. McFadden,[a] Nicole Moon,[b] Frank E. Marshall,[b] Amanda J. Duerden,[b] Esther J. Ocola,[c] Jaan Laane,[c] Gamil A. Guirgis[a] and G. S. Grubbs II *[b]

Received 19th September 2021,
Accepted 7th January 2022

DOI: 10.1039/d1cp04286f

rsc.li/pccp

The molecules 1,1-difluorosilacyclopent-3-ene ($3SiCPF_2$) and silacyclopent-3-ene (3SiCP) have been synthesized and studied using chirped pulse, Fourier transform microwave (CP-FTMW) spectroscopy. For 3SiCP this is the first ever microwave study of the molecule and, for $3SiCPF_2$, the spectra reported in this work have been combined with that of previous work in a global fit. The spectra of each contain splitting which has been fit using a Hamiltonian consisting of semirigid and Coriolis coupling parameters. A refit of the original $3SiCPF_2$ work was also carried out. All fits and approaches are reported. Analyses of the spectra provide evidence that the molecule is planar which is in agreement with the high-level calculations, but the source of the splitting in the spectra has not been determined.

Introduction

The ring-puckering vibrations of four-membered ring and "pseudo-four-membered ring" molecules, such as cyclopentene, have been experimentally investigated by far-infrared, Raman, and microwave spectroscopy[1–9] for more than half a century. Interest in this vibration arose after R. P. Bell[10] predicted that the potential energy function (PEF) for this motion in a four-membered ring should be quartic in nature. This proved to be mostly true although Laane[9] in 1971 showed that the PEF would be of the form

$$V(x) = ax^4 + bx^2 \quad (1)$$

The constant a arises primarily from angle strain forces while b derives from both torsional and angle strain interaction. This is the case for both four-membered and pseudo-four-membered ring molecules. The ring-puckering coordinate for the latter type is shown in Fig. 1 for cyclopentene.

The great interest in determining the one-dimensional PEF shown in eqn (1) has not only been to demonstrate that the quantum mechanical solution works extremely well, but also to provide insight into the conformations and intramolecular forces of these molecules. Cyclopentene was the first pseudo-four-membered ring to be studied,[11] and it was shown to be a puckered molecule with a negative b coefficient and a barrier to planarity of 232 cm^{-1}. The barrier was due to CH_2–CH_2 interactions.

In our present study we will report our microwave results for 1,1-difluorosilacyclopent-3-ene ($3SiCPF_2$) and silacyclopent-3-ene (3SiCP). These results are complemented by high level theoretical calculations. The far-infrared spectra of 3SiCP[12] were reported in 1969 and the Raman spectra[13] in 1975. Vibrational assignments[14] were reported in 1972, molecular mechanics calculations[15] in 1989, and theoretical calculations in 2014.[16] Laane has performed a 2D ring puckering/twisting potential for 3SiCP,[17] while Al-Saadi[18] has performed ring puckering calculations for both and 3SiCP and $3SiCPF_2$. Microwave results have previously been

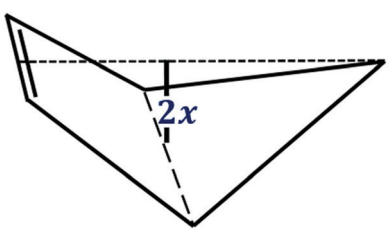

Fig. 1 Definition of ring puckering coordinate, x, for cyclopentene and related molecules.

[a] Department of Chemistry and Biochemistry, College of Charleston, 66 George Street, Charleston, South Carolina 29424, USA
[b] Department of Chemistry, Missouri University of Science and Technology, 400 West 11th Street, Rolla, Missouri 65409, USA. E-mail: grubbsg@mst.edu
[c] Department of Chemistry and Institute for Quantum Science and Engineering, Texas A&M University, College Station, Texas 77843, USA

† Electronic supplementary information (ESI) available. See DOI: 10.1039/d1cp04286f

reported for $3SiCPF_2$,[19] but 3SiCP has not been previously studied. In addition, gas phase electron diffraction results have been previously reported for both $3SiCPF_2$ and 3SiCP.[20] All work on 3SiCP and $3SiCPF_2$ are consistent that the molecular ring is planar and the potential energy constant *b* in eqn (1) is small.

We have recently reported the microwave and theoretical work on 1,1-difluorosilacyclopent-2-ene[21] ($2SiCPF_2$). This molecule's experimental (ground state) and theoretical (equilibrium) structure was determined to be planar, with a small, but positive value for the potential energy constant, *b*.

Experimental

The two title compounds were synthesized at the College of Charleston. All reagent transfers and reactions were carried out under an atmosphere of argon or *in vacuo* using standard Schlenk techniques. Solvents were dried with lithium aluminum hydride, stored under argon, and were distilled immediately prior to use. Antimony trifluoride was purified *via* sublimation, and all other reagents were used as received. ^{1}H, ^{13}C, ^{19}F, and ^{29}Si NMR spectra were obtained using a Bruker 400 MHz NMR spectrometer. NMR chemical shifts were referenced to solvent peaks as internal standards and coupling constant errors were typically about 0.2 Hz.

Synthesis of $3SiCPF_2$

A 20 cm Schlenk tube with a vacuum adapter was equipped with a stir bar, and 1,1-dichlorosilacyclopent-3-ene (4.00 g, 26.3 mmol) was added to the tube. The compound was frozen with liquid nitrogen and antimony trifluoride (4.68 g, 26.3 mmol) was added to the tube while purging with argon. The reaction mixture was frozen with liquid nitrogen, evacuated to 0.10 torr, and closed. The reaction mixture was heated to 55 °C for 1 h while stirring. The product was collected and purified by separating volatile components on a temperature gradient under reduced pressure (0.10 torr). The product was collected in a liquid nitrogen trap after passing through a trap at −65 °C. A total of 1.67 g, 13.9 mmol of purified 1,1-difluoro-1-silacyclopent-3-ene was collected. Yield: 53%. ^{1}H NMR (400 MHz, $CDCl_3$): δ (ppm) 6.00 (tt, 4.6 and 1.2 Hz, 2H, =C–H) 1.43 (m, 3.6 and 1.2 Hz, 4H, CH_2). ^{13}C NMR (400 MHz, $CDCl_3$): δ (ppm) 129.38 (t, 4.0 Hz), 11.36 (t, 15.0 Hz). ^{19}F NMR (400 MHz, $CDCl_3$): δ (ppm) −139.52 (m, 3.7). ^{29}Si NMR (400 MHz, $CDCl_3$): δ (ppm) 14.84 (t, 323.0 Hz).

Synthesis of 3SiCP

Into a 250 mL Schlenk flask equipped with a stir bar was added 1,1-dichlorosilacyclopent-3-ene (20.0 g, 13.2 mmol) in 100 mL of dibutyl ether. The solution was brought to −15 °C and lithium aluminum hydride (1.00 g, 26.4 mmol) was added directly to the flask while purging with argon. The mixture stirred for one hour and the cold bath was removed. After the reaction mixture warmed to rt and stirred for 1 h, the progression of the reaction was checked using ^{1}H NMR spectroscopy. Upon completion, volatile components were vacuum transferred to a second 250 mL Schlenk flask. The flask containing vacuum transferred solvent and product was purified by separating components based on vapor pressure through cold traps under reduced pressure (0.12 torr). The traps were kept at −55 °C, −70 °C, and the temperature of boiling liquid nitrogen (−196 °C). The purified product was collected in the liquid nitrogen trap, and solvent and side products were collected in the other two traps. A total of 6.85 g, 81.6 mmol of purified product was isolated. Yield: 62% (Scheme 1). ^{1}H NMR (400 MHz, $CDCl_3$): δ (ppm) 5.93 (s, 2H, =C–H), 3.97 (s, 2H, SiH_2), 1.54 (s, 4H, CH_2). ^{13}C NMR (400 MHz, $CDCl_3$): δ (ppm) 131.14, 11.74. ^{29}Si NMR (400 MHz, $CDCl_3$): δ (ppm) −27.69.

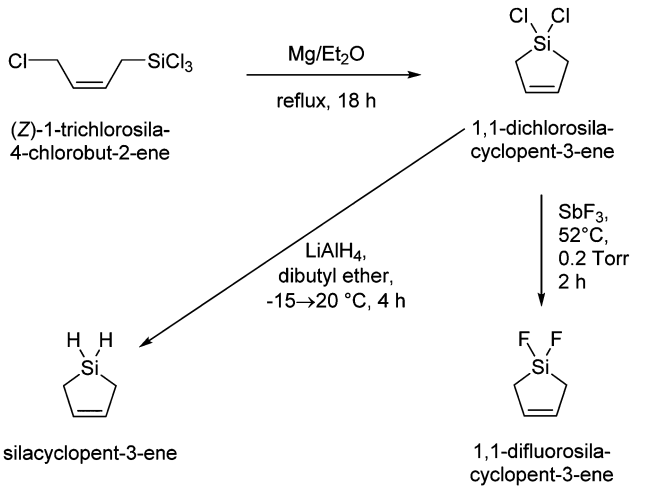

Scheme 1 Synthesis processes for 3SiCP and $3SiCPF_2$.

Microwave spectroscopy

Microwave experiments were performed at Missouri S&T using a chirped-pulse, Fourier transform microwave (CP-FTMW) spectrometer. This spectrometer has been detailed in the literature elsewhere.[22–26] In the current work, the spectrometer was used in the traditional setup without using multi-antenna detection.[26] Spectra were obtained using 4 μs chirps in separate 6–12 and 12–18 GHz scans. Each scan consisted of the supersonic nozzle being pulsed at 5 Hz with 5, 20 μs free induction decays (FIDs) being collected with each gas pulse until the sample was consumed. For $3SiCPF_2$, 99 900 FIDs were collected and averaged in each scan while 70 000 and 60 000 FIDs were collected for the 6–12 and 12–18 GHz scans of 3SiCP, respectively. The resultant scans for each molecule are presented in Fig. 2 and 3. The FIDs were averaged in the time domain and Fourier transformed using Kisiel's FFTS[27] software with the default Bartlett window. Using these parameters, typical linewidths have full-width, half maximum (FWHM) values of 60–80 kHz unless otherwise broadened (unresolved splitting, *etc.*) with an attributed 10 kHz uncertainty in the line centers.

Before spectra were acquired, individual tanks containing 3% $3SiCPF_2$ and 3% 3SiCP diluted in Ar were prepared. The resulting samples were introduced into the spectrometer's vacuum chamber (held at 10^{-6} torr) using an absolute pressure of 500 torr (−260 torr relative) through a standard Parker-Hannifin® Series 9 solenoid valve with 0.8 mm orifice.

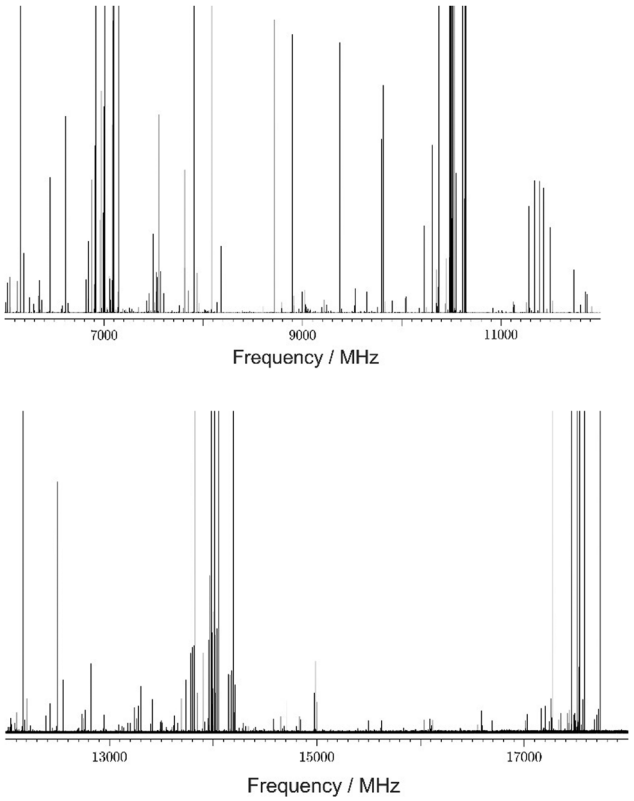

Fig. 2 The 6–12 (top) and 12–18 (bottom) GHz spectrum of $3SiCPF_2$. The most intense transitions have been cut off in order to see less intense transitions.

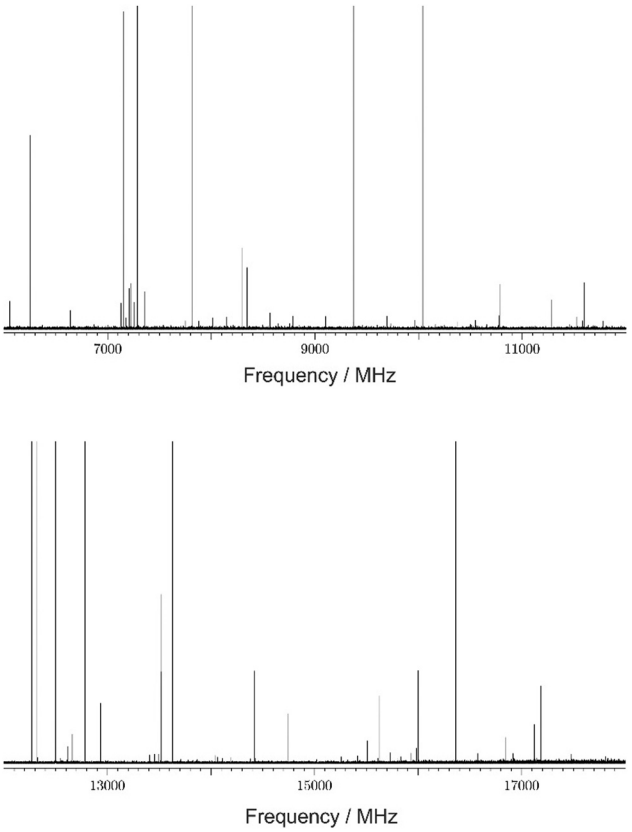

Fig. 3 The 6–12 (top) and 12–18 (bottom) GHz spectrum of 3SiCP. The most intense transitions have been cut off in order to see less intense transitions.

Quantum chemical calculations

Structure calculations

The geometrical structures, rotational constants and potential energies of diverse conformations of $3SiCPF_2$ and 3SiCP were calculated using CCSD/cc-pVTZ *ab initio* computations at Texas A&M University. The Gaussian 16 program[28] was used for the computations, and the GaussView 6.1.1 graphical interface[29] was used to visualize the structures.

The calculated geometrical structures of $3SiCPF_2$ and 3SiCP are shown in Fig. 4 and the principal rotational constants and dipole moments for these structures are reported in Table 1. The labelling of the carbon atoms is also indicated in the figure. As can be seen, one effect of substituting the electronegative halide atoms is to shorten the Si–C bonds. The C–Si–C angles are increased by about 2.4 degrees in the dihalide. The F–Si–F angle is about 2.6 degrees smaller than the H–Si–H angle. The other bonds and bond angles are much less affected and have typical magnitudes for Si–C, C–C, and C═C bonds.

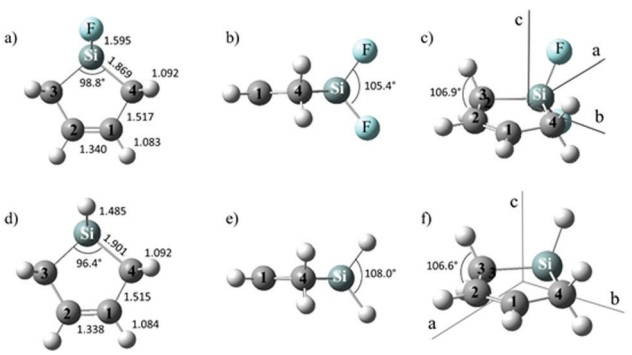

Fig. 4 (a–c) Calculated structural parameters of $3SiCPF_2$ and (d–f) 3SiCP in their minimum energy conformations from CCSD/cc-pVTZ computations. The bond distances are in Ångströms (Å). The principal rotation axes *a*, *b* and *c* are shown in (c) and (f).

Kinetic energy and potential energy calculations

The quantum mechanical problem has the form

$$\frac{-\hbar^2}{2}\frac{\partial}{\partial x}g_{44}(x)\frac{\partial}{\partial x}\Psi(x) + V(x)\Psi(x) = E\Psi(x) \qquad (2)$$

where V is given in eqn (1). The Laane ASYMNEW program[30] based on vector and numerical methods was used to calculate the coordinate dependent kinetic energy functions for both molecules. The geometrical parameters for the computed planar structures of these molecules provided the input for the program. The reciprocal reduced mass functions $g_{44}(x)$ were calculated with a dependence on the puckering coordinate x (subscripts 1 to 3 on g are reserved for the molecular rotations).

The conformational energies V *vs.* x were calculated for 10 and 12 values of the ring-puckering coordinate of $3SiCPF_2$ and

Table 1 Theoretically calculated rotational constants for $3SiCPF_2$ and 3SiCP at the CCSD/cc-pVTZ level

	c-$C_4H_6{}^{28}SiF_2$	c-$C_4H_6{}^{28}SiH_2$
A/MHz	3522.5	5937.3
B/MHz	1780.3	4515.2
C/MHz	1690.6	2731.0
$\|\mu_a\|$/D	2.19	0.31
$\|\mu_b\|$/D	0.00	0.00
$\|\mu_c\|$/D	0.00	0.00

3SiCP, respectively. Using Maple software[31] this data was then used to determine the potential energy parameter a and b in eqn (1) in order to produce the theoretical PEF. The DA1OPTN Meinander–Laane potential energy program[32] was used to calculate the energy levels and the energy level spacings of $3SiCPF_2$.

The Hermite polynomial coefficients of the wavefunctions for the potential energy functions were calculated using the DA1OPTN Meinander–Laane potential energy program.[32] The wavefunctions were calculated using MAPLE 2015.1 computing environment.[31]

A principal aim of this investigation was to understand the energetics of the ring-puckering vibration of $3SiCPF_2$. The one-dimensional quantum mechanical expression we utilized for this study is given in eqn (2) and the form of the PEF is given in eqn (1). Using the geometrical parameters from the CCSD/cc-pVTZ computations, the kinetic energy functions for $3SiCPF_2$ was calculated.

This is given by

$$g_{44}(x) = 4.143 \times 10^{-3} - 1.750 \times 10^{-2}x^2 - 1.421 \times 10^{-2}x^4 - 1.281 \times 10^{-1}x^6. \quad (3)$$

The corresponding calculated reduced mass for the ring-puckering for 3SiCPF2 is 241.4 u.

The calculated PES that fitted to the calculated potential energies for 10 different configurations of $3SiCPF_2$ is given by

$$V_{3SiCPF_2}(cm^{-1}) = 2.139 \times 10^5 x^4 + 5.865 \times 10^3 x^2. \quad (4)$$

Fig. 5 shows the calculated PES, lowest ring-puckering transitions, energy levels and wavefunctions for $3SiCPF_2$. Fig. 6 shows the experimentally fit PES for 3SiCP previously determined by the Laane research group in 2014.[16] Our calculated wavefunctions for this molecule are also shown. As mentioned previously, the FIR transitions were observed and reported by Laane in 1969.[12]

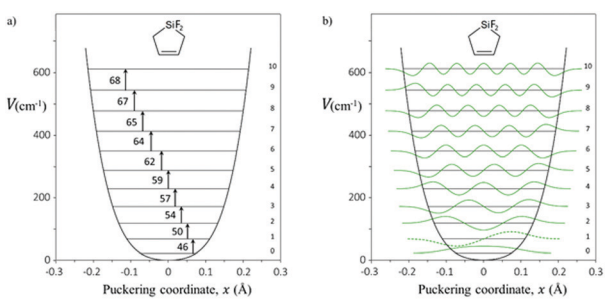

Fig. 5 (a) Theoretical ring-puckering PEF for $3SiCPF_2$. The calculated transitions are also shown. (b) Calculated wavefunctions for the lower energy levels. The molecule is calculated to be planar.

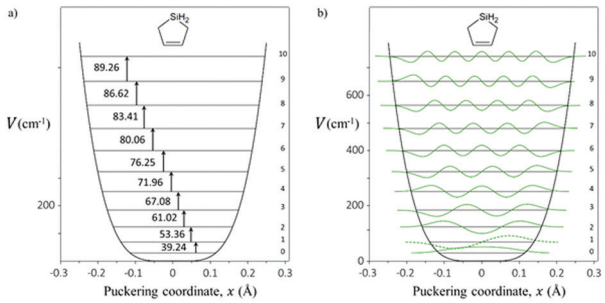

Fig. 6 (a) Experimentally fit ring-puckering PEF for 3SiCP. The calculated transitions are also shown in the figure. (b) Calculated wavefunctions for the lower energy levels. The molecule is calculated to be planar.

Fig. 7 shows a comparison of the ring-puckering PEFs for $3SiCPF_2$ and the hydride 3SiCP. The potential energy constant for eqn (1) and the calculated reduced masses for each are given in Table 2. $3SiCPF_2$ is calculated to be slightly more rigid than 3SiCP.

Results and discussion

Assignment

Assignments were performed on both $3SiCPF_2$ and 3SiCP using Pickett's SPFIT/SPCAT[33] program suite in conjunction with Kisiel's AABS[34] software front-end. Both molecules were fit using a Watson S-reduced Hamiltonian in the I^r representation.[35] Rotational constants and quartic centrifugal distortion constants D_J and D_{JK} were needed to adequately describe each data set. All assignments and fit files have been reproduced in a easily read format using PIFORM[36] and may be found in the ESI.†

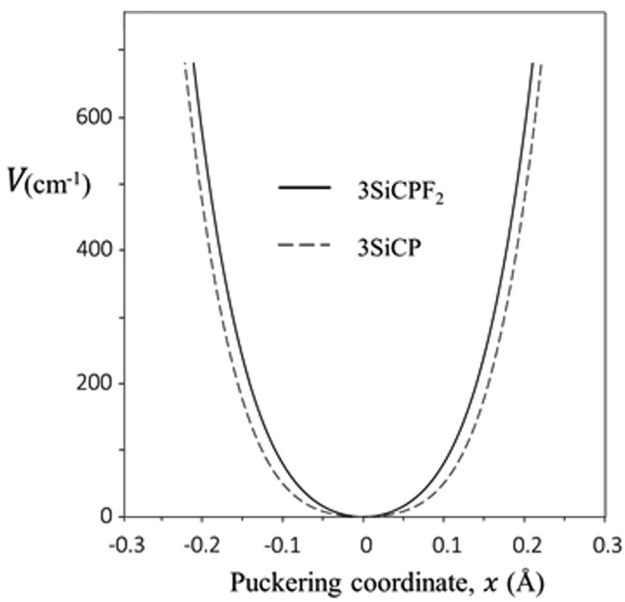

Fig. 7 Comparison of calculated PEFs for $3SiCPF_2$ and 3SiCP from CCSD/cc-pVTZ computations.

Table 2 Potential energy parameters[a] for $3SiCPF_2$ and 3SiCP using $V = ax^4 + bx^2$

Molecule	Reduced mass/u	a	b	Barrier, cm^{-1}
$3SiCPF_2$[b]	241.40	2.139×10^5	5.865×10^3	0
3SiCP[b]	127.84	2.273×10^5	2.751×10^3	0
3SiCP[c]	128.64	2.130×10^5	-0.054×10^4	0.3
3SiCP[d]	*158.44*	2.089×10^5	2.810×10^2	0

[a] Units for a are cm^{-1} Å^{-4}; units for b are cm^{-1} Å^{-2}. The reduced mass is in atomic units. [b] From CCSD/cc-pVTZ computations. [c] From ref. 12. The PEF was experimentally fit according to an estimated reduced mass reported in 1969. [d] From ref. 16. The PEF was experimentally fit according to the calculated reduced mass reported in ref. 17.

Assignments began with $3SiCPF_2$ because the previous work by Durig and Laane[19] provided rotational constants and dipole moments for the parent species in the ground vibrational state. The values reported were $A = 3546.36 \pm 1.40$ MHz, $B = 1798.07 \pm 0.02$ MHz, and $C = 1706.25 \pm 0.02$ MHz and $|\mu_a| = 2.02 \pm 0.06$ D, $|\mu_b| = 0$ D, and $|\mu_c| = 0.00 \pm 0.09$ D. This agreed well with our calculated values presented in Table 1 providing additional confidence for their use. As expected, this greatly simplified assignment as we were able to input these values directly into SPCAT and predict transitions accurately. From there the relative "correct intensity" feature of the spectrometer was utilized as the predicted intensities matched very well with prediction.[37] Once enough transitions were added, however, we were able to update the fit to utilize semirigid Watson S-reduced terms, not previously included because of this species being reported on prior to their complete development.[35] *R*- and *Q*-branch, *a*-type transitions, in accordance with dipole moment values, were assigned.

During the assignment of $3SiCPF_2$, some, but not all, transitions presented as doublets (see Fig. 8) or were broadened significantly from the typical 60–80 kHz FWHM transitions linewidth. In addition to this, centrifugal distortion constants began to grow unreasonably large for an otherwise large ring molecule. Both of these are strong indicators of a motion in the molecule leading to a splitting in vibrational ground state. In order to verify that this was the case, and these indicators were not being misinterpreted, two sets of fits were undertaken where split transitions were taken into account. One where the spectra were fit to two different sets of rotational constants and another where they were fit to singular set of rotational constants. In SPFIT/SPCAT, motions of the molecule resulting in splitting are fit using vibrational states as labels. Therefore, $v = 0$ and $v = 1$ correspond to concepts such as A and E of a methyl rotor or + and − of a ring-twisting/puckering motion.

The two fits are reported in Table 3. In each, one rotation-vibration parameters, F_{bc} was required. This correspond to Coriolis parameter F_a as described by Pickett.[38] Because we had trouble isolating the source of the splitting (see Curious motions section), it isn't entirely clear as to where this term arises, but adequate fits cannot be obtained without the term being included in each of the fitting approach. ΔE_{01} is also necessary to account for the differences between the two states. Although fitting this type of spectra is described as a tunnelling motion in Pickett, it is fit using vibrational states as labels. Also, when these terms were added, centrifugal distortion parameters decreased to more reasonable values; being on the order of similar silicon-ring molecules. Due to the agreement between methods, the limited data set of transitions, and the fact that not all transitions presented as doublets, it was determined to proceed with a single set of rotational constants in all minor isotopologue fits.

All singly-substituted minor isotopologue spectra of $3SiCPF_2$ were observed and fit for the first time. These fits are presented in Table 4. Assignments were aided by using the rotational constants generated from the theoretical structure for the different isotopologues and adjusting these values based on the ratios between the parent experimental-to-theoretical A, B, and C values. Doubling was present again in the silicon isotopologues, but there was no doubling observed in the

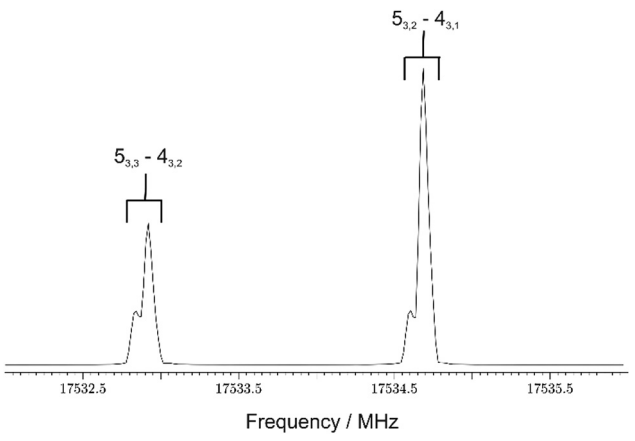

Fig. 8 An example of splitting observed in the $3SiCPF_2$ spectrum during assignment. The spectra shown are for the $J'_{Ka,Kc} - J''_{Ka,Kc} = 5_{3,3}-4_{3,2}$ and $5_{3,2}-4_{3,1}$ transitions. Splitting appears as "shoulders" on the transitions at this resolution.

Table 3 Spectroscopic parameters of the parent isotopologue of $3SiCPF_2$. The fits are in excellent agreement when performed together and separately[a]

		Fit separate	
Parameter	Fit together	$v = 0$	$v = 1$
A/MHz	3544.4280(35)[b]	3544.4239(30)	3545.87 (56)
B/MHz	1798.1391(23)	1798.1419(23)	1798.1316(45)
C/MHz	1706.3013(25)	1706.2988(27)	1706.3085(29)
D_J/kHz	0.162(40)	0.201(36)	
D_{JK}/kHz	5.82(14)	5.87(13)	
F_{bc}/MHz	0.86(13)	0.68(16)	
ΔE_{01}/MHz	11 800(1410)	13 010(720)	
RMS[c]/kHz	16.6	11.8	
N[d]	38	26	12

[a] See text for details. [b] Values in parentheses for the literature values are the reported uncertainties given in units of the least significant figure. Values in parentheses for the fitted rotational constants are the 1σ uncertainties (67% confidence interval) given in units of the least significant figure. [c] Microwave RMS $\left(\sqrt{\left(\sum\left[(\text{obs}-\text{calc})^2\right]/N\right)}\right)$. [d] Number of transitions.

Table 4 Spectroscopic parameters of the minor isotopologues of $3SiCPF_2$. Split transitions were observed and assigned for the silicon-30 and silicon-29 species, but not for the carbon-13 species

Parameter	^{30}Si	^{29}Si	^{13}C (3 & 4)	^{13}C (1 & 2)
A/MHz	3544.41(37)[a]	3543.45(47)	3494.65(29)	3533.34(33)
B/MHz	1794.5529(25)	1796.3240(36)	1795.3127(22)	1773.2146(22)
C/MHz	1703.0745(24)	1704.6780(36)	1692.4510(22)	1681.4202(20)
D_J/kHz	0.245(39)	0.223(58)	0.258(37)	0.181(36)
D_{JK}/kHz	5.42(15)	5.73(16)	5.32(17)	5.08(11)
F_{bc}/MHz	0.50(32)	0.86(19)	—	—
ΔE_{01}/MHz	8390(1460)	11 480(1350)	—	—
RMS[b]/kHz	20.1	24.5	15.2	14.3
N[c]	27	28	22	22

[a] Values in parentheses for the literature values are the reported uncertainties given in units of the least significant figure. Values in parentheses for the fitted rotational constants are the 1σ uncertainties (67% confidence interval) given in units of the least significant figure. [b] Microwave RMS $\left(\sqrt{\left(\sum\left[(\text{obs}-\text{calc})^2\right]/N\right)}\right)$. [c] Number of transitions.

weaker ^{13}C species. In accordance with theory, only two sets of parameters were possible for all ^{13}C isotopologues as carbons 1 and 2 and 3 and 4 were spectroscopically equivalent. In total, 99 transitions were observed for the singly-substituted species in the spectral region.

The next molecule to be fit was 3SiCP. In accordance with $3SiCPF_2$, only R- and Q-branch, a-type transitions were observed. These spectra, as shown in Fig. 3, were considerably weaker and less dense than that of $3SiCPF_2$. Both of these observations agreed well with the dipole moments and rotational constants' magnitudes from theory. Due to the spectra being less intense, only the parent, ^{30}Si, and ^{29}Si species were observed before all sample was exhausted. Table 5 reports the fitted parameters for all observed isotopologues. The theoretical rotational constants provided excellent starting points for assignment as the prediction generated by SPCAT and output by AABS were closely matched. As mentioned previously, a Watson S-reduced Hamiltonian in the I^r representation was used. This time, however, all quartic centrifugal distortion constants were determined. As also was the case of $3SiCPF_2$, doubling was observed in the spectra. Again, only the F_{bc} Coriolis parameter and ΔE_{01} were needed for assignment. There were not enough intense transitions to observe the doubling on the minor isotopologues, however, so they were fit without the Coriolis terms and holding the centrifugal distortion terms to the parent values. A total of 27 transitions were observed for the parent while 4 were observed for the ^{30}Si and ^{29}Si isotopologues.

Table 5 Spectroscopic parameters for all isotopologues of 3SiCP. Split transitions were observed and assigned for the parent only

Parameter	Parent	Silicon-29	Silicon-30
A/MHz	5948.1093(47)[a]	5947.902(40)	5949.02(13)
B/MHz	4538.2601(39)	4509.5059(39)	4460.985(38)
C/MHz	2748.4793(41)	2717.0641(39)	2694.090(18)
D_J/kHz	0.71(11)	[0.71][b]	[0.71]
D_K/kHz	1.18(25)	[1.18]	[1.18]
d_1/kHz	−0.340(38)	[−0.340]	[−0.340]
d_2/kHz	−0.111(21)	[−0.111]	[−0.111]
F_{bc}/MHz	6.06(15)	—	—
ΔE_{01}/MHz	131812(381)	—	—
RMS[c]/kHz	23.1	5.2	16.5
N[d]	27	4	4

[a] Values in parentheses for the literature values are the reported uncertainties given in units of the least significant figure. Values in parentheses for the fitted rotational constants are the 1σ uncertainties (67% confidence interval) given in units of the least significant figure. [b] Values in brackets are held to the determined parent values. [c] Microwave RMS $\left(\sqrt{\left(\sum\left[(\text{obs}-\text{calc})^2\right]/N\right)}\right)$. [d] Number of transitions.

Refits and global fits

As mentioned prior, the previous work by Durig and Laane[19] provided a great starting point for the $SiCPF_2$ fits reported here. However, there were two aspects of our work that didn't agree well with the prior work or made comparisons inequivalent. Those were that the authors reported not observing any splitting of transitions and that this work happened prior to the development of Watson's semirigid Hamiltonians, so that there were no centrifugal distortion terms with which to compare while also directly affecting the reported rotational constants as they will adjust accordingly to best-fit the data set. Because it is important to understand our data in the context of all microwave data available, we embarked on working with the previously measured transitions in order to add our data and produce global fits for the entire data set. All fits have been reproduced in an easily read format using PIFORM[36] and may be found in the ESI.†

The first goal, then, was to reproduce the fits of Durig and Laane[19] to be sure that the transitions didn't have any obvious reporting (*i.e.* typographical) errors. Using SPFIT and only the assigned transition states, then, we reproduced fits of rotational constants only for all vibrational states reported. These are found in Table 6 as a comparison of the reported literature values (top portion of the table) with our fitted values from their reported transitions (bottom portion of the table).

Table 6 Refit of the $3SiCPF_2$ rotational constants from Durig and Laane[a]

Vibrational state	A/MHz	B/MHz	C/MHz
Literature values			
$v = 0$	3546.36(140)[b]	1798.07(2)	1706.25(2)
$v = 1$	3543.54(200)	1801.89(4)	1714.02(2)
$v = 2$	3542.17(240)	1805.19(19)	1720.47(4)
$v = 3$	3539(3)	1808.01(20)	1726.22(4)
Rotational constants from literature transitions[c]			
$v = 0$	3546.1(14)	1798.070(14)	1706.247(13)
$v = 1$	3543.6(20)	1801.878(40)	1714.021(15)
$v = 2$	3542.2(23)	1805.19(18)	1720.470(39)
$v = 3$	3830(103)	1811.7(12)	1724.87(43)

[a] See text for details. [b] Values in parentheses for the literature values are the reported uncertainties given in units of the least significant figure. Values in parentheses for the fitted rotational constants are the 1σ uncertainties (67% confidence interval) given in units of the least significant figure. [c] Microwave RMS $\left(\sqrt{\left(\sum\left[(\text{obs}-\text{calc})^2\right]/N\right)}\right)$ and number of transitions for rotational constant fits: $v = 0$, RMS = 0.336 MHz, $N = 22$; $v = 1$, RMS = 0.204 MHz, $N = 9$; $v = 2$, RMS = 0.167 MHz, $N = 7$; $v = 3$, RMS = 0.018 MHz, $N = 4$.

As expected, our values overall agree very well with those reported with the largest discrepancies coming from the A rotational constant which is the most difficult to determine using small data sets of only a-type transitions. This is especially true for the $v = 3$ state where only four (4) transitions were reported. This state also (unsurprisingly) had the largest discrepancies with our refit of the data. Due to this excellent agreement, particularly in the $v = 0$ state which would be used for our global fits, we proceeded forward.

In order to do our best not to bias any conclusions, we started the global fits by setting the transitions observed in the Durig and Laane[19] work $v = 0$ state to our $v = 0$ (lower state of a the splitting) and added the transitions to our parent transition listing holding the Coriolis terms to our originally determined values. This brought the new number of transitions to 60 and extended the frequency range of measured transitions to 39 GHz. 50 kHz uncertainty was given to these transitions as had been done in the previous work. The results are presented in Table 7 as ''Holding Coriolis'' alongside our other global fit approaches. A listing of the quantum number assignments and formatted fit files for all global fits using PIFORM on SPFIT .fit files may be found in the ESI.† As was needed for our data set alone, D_J and D_{JK} were determinable and in good agreement with our determined values, but all other quartic centrifugal distortion were not determinable, even with the extended data set.

As can be observed from Table 7, however, the Microwave RMS of this approach was 163 kHz, over 6×'s that of the average error attributed to the uncertainties. A quick scan of the obs − calc showed that a few transitions from the previous work were being assigned to states that were well away from where they were being predicted. However, when we produced predictions using SPCAT, they were much closer to other quantum number assignments; including those which corresponded to our $v = 1$ (splitting) state. These transitions were adjusted where applicable and a new fit was produced, still holding the fit to our original Coriolis values. This fit is labelled ''Adjusted Transitions'' in Table 7 to reflect the Coriolis being held and only the transitions were adjusted. This time D_K was determinable in addition to D_J and D_{JK} and the Microwave RMS was reduced from 163 to 51.6 kHz.

Although this was significant improvement from the ''Holding Coriolis'' global fit, as mentioned previously, such a large magnitude in the value for D_K (−200 kHz) could be an indicator that the Coriolis terms need refinement in the fit. As a complete analysis, then, we let all parameters adjust in the final fit labelled ''Fit Coriolis'' in Table 7. This fit again lowered the Microwave RMS to 49.1 kHz, which is a true RMS of approximately 1.6, which agrees well with our data without Durig and Laane's transitions (true RMS of 2.15). Another notable aspect is that D_K was undeterminable, as it was with our previous data set, and the rotational constants, as well as the remaining D_J and D_{JK}, values agree very well with our data set's determined values. It should be noted that F_{bc} and ΔE_{01} are not significantly different (*i.e.* they are within error) from our previously determined values for these parameters and became better determined. Taking all of the information into account, we surmise that the ''Fit Coriolis'' best represents the data set but suggest that spectroscopic work on $3SiCPF_2$ at higher frequencies – for which we don't have access – would help to provide more information toward this conclusion.

Table 7 Global fits of $3SiCPF_2$ transitions with those from Durig and Laane[a]

Parameter	Holding Coriolis	Adjusted transitions	Fit Coriolis
A/MHz	3544.4281(60)[b]	3543.62(45)	3544.4249(38)
B/MHz	1798.1390(32)	1798.1370(19)	1798.1388(19)
C/MHz	1706.3031(31)	1706.3029(20)	1706.3012(19)
D_J/kHz	0.191(24)	0.186(19)	0.165(15)
D_{JK}/kHz	5.75(17)	5.61(11)	5.76(10)
D_K/kHz	—	−200(113)	—
F_{bc}/MHz	[0.86][c]	[0.86]	0.807(97)
ΔE_{01}/MHz	[11 800]	[11 800]	12 430(370)
RMS[d]/kHz	163	51.6	49.1
N[e]	60	60	60

[a] See text for details. [b] Values in parentheses for the literature values are the reported uncertainties given in units of the least significant figure. Values in parentheses for the fitted rotational constants are the 1σ uncertainties (67% confidence interval) given in units of the least significant figure. [c] Values in brackets are held. For exact held values, see the ESI. [d] RMS is defined as $\sqrt{\left(\sum\left[(\text{obs}-\text{calc})^2\right]/N\right)}$ where N is the number of transitions. [e] Number of transitions.

Structure of $3SiCPF_2$ and 3SiCP

One very important aspect of the chemistry and spectroscopy of silicon-containing ring molecules concerns their structure. Especially with regards to their fully carbonated counterparts. Because there was a significant amount of isotopic data available, as well as a significant amount of data for comparison, we embarked on developing experimental ring-structure analysis for the $3SiCPF_2$. The first approach utilized Kraitchman substitution structures.[39] Given the small amount of data for 3SiCP molecules, however, a Kraitchman analysis might not be very meaningful. The Kraitchman analysis for $3SiCPF_2$ only, then, is presented in Table 8.

The first notable item from the Kraitchman analysis is that the c-coordinate has nonzero values for all atomic substitutions except for ^{30}Si, where it is effectively zero. This, however, does not agree well with our theoretical and previous theoretical

Table 8 Kraitchman[39] substitution coordinates for $3SiCPF_2$[a]

Atom	a/Å	b/Å	c/Å
^{29}Si	0.5153(97)[b]	0.137(36)[c]	0.145(35)[c]
^{30}Si	0.5345(45)	0.008(310)[d]	0.018(140)[d]
^{13}C (1/2)	−1.9874(19)	±0.6741(56)	−0.090(43)[c]
^{13}C (3/4)	−0.6431(52)	±1.4209(24)	0.168(22)[c]

[a] Kraitchman analyses only give magnitudes. Signs reported have been assigned in accordance with their theoretical values. [b] Numbers in parentheses represent the Costain errors[42] in the least significant figure. [c] Theoretical value is 0.00 Å for this coordinate. Therefore, sign has been assigned based on most reasonable value. [d] Reported values of zero are where the Kraitchman substitution method returned an imaginary result.

work on the molecule.[18] To reconcile this inconsistency, then, it was important to compare the structural implications of these positions as well as understand the nature of the Kraitchman analysis and its pitfalls, especially when comparing to equilibrium structures. Due to the way the Kraitchman analysis is performed, substitution structures from this analysis method have been known to have problems with atomic positions close to a zero value for a coordinate. In other works,[40] the authors have utilized the double substitution method of Rudolph[41] in order to arrive at more reasonable values for molecular geometries. In this work, this is noticeable from the large error in this coordinate for the ^{30}Si substituted species.

Because only singly substituted data were available, however, we had to take a different approach for $3SiCPF_2$. To investigate further, we input the Kraitchman coordinates into Kisiel's EVAL program on the PROSPE website.[36] This provided a unique set of r_S parameters for substituting the ^{29}Si and ^{30}Si independently. These parameters are compared to the r_e values from our equilibrium structure and the electron diffraction work of Rankin and coworkers[20] in Table 9. As we are both attempting to get the best experimental structure and determine the shape of the ring, the best comparator is to look at the Si–C bond lengths as they should be largely consistent across a number of molecules and geometries and match well with theory. There is an obvious outlier in the group with the ^{29}Si structure having vastly different Si–C_3 and Si–C_4 bond lengths both compared within itself and across the different methods. This was a good indicator that Kraitchman was probably not doing a good enough job with the structure derived from this isotopologue. The structure derived from ^{30}Si, however, showed great consistency and agreement both with all Si–C bonds in the structure and with the calculated and electron diffraction structure, so we will use that structure as our best experimental r_S structure.

Settling on the ^{30}Si Kraitchman coordinate as the basis for the r_S, the r_e, r_S, and electron diffraction ring structure parameters are in excellent agreement with one another with one exception, the dihedral angle formed from the double bond carbons, an adjacent carbon, and the silicon atom (listed as the $C_1{=}C_2{-}C_3{-}Si$ angle in Table 9). In the electron diffraction work, this is defined as δ and determined to be 13.9(8)°.[20] This value is in excellent agreement (at least in magnitude) with our value of −11.6(60)°. In the electron diffraction work, this angle is attributed to a low amplitude ring-shrinkage deformation vibration. This seems to be plausible as explained in the Curious motions subsection immediately following this structure discussion.

Because the Kraitchman substitution approach wasn't entirely conclusive and there has yet to be any discussion of the 3SiCP molecule, we decided to utilize Bohn's method of planar moment analysis to arrive at conclusions for the experimental structure.[43] This method takes advantage of similarities in functionalization to provide fundamental insights regarding structure. The advantage to using it here is that we are able to utilize the most determined set of parameters – those for the parent $3SiCPF_2$ and 3SiCP isotopologues – as our basis for comparison. Second moments for $3SiCPF_2$, 3SiCP and similar molecules 1,1-difluorosilacyclopent-2-ene ($2SiCPF_2$),[21] 1,1-difluorosilacyclopentane ($SiCPF_2$),[44] and silacyclopentane (SiCP)[45] are presented in Table 10.

In order to interpret structure using Table 10 care must be taken in order to make comparisons within a family. First of all, halogen substitution will cause shifts in the principal axis system, so it is easiest to make comparisons among species with the equal substitution above and below the ring (fluorination above and below the ring or completely halogenated). Table 10 has been organized in this way. Ring planarity in all of these molecules moves mass out of the *ab*-plane and into the *ac*-plane, therefore we can monitor ring planarity by a comparison of the P_{bb} (out-of-*ac*-plane mass) and P_{cc} (out-of-*ab*-plane mass) values. We will focus on P_{bb} here because the halogenation makes P_{cc} values change dramatically while P_{bb} is very consistent, allowing us to make comparisons amongst the entire family.

Inspection of P_{bb} in Table 10 shows that the values range from 77.69–83.04 amu Å^2 across the family. This may not seem like very much, but, investigating further, it is noticed that the species determined to be nonplanar – SiCP and $SiCPF_2$ – both have values above 80 amu Å^2. This is because whereas change in position of the double bond may slightly affect where the axis system lies, it will only do so by about 1 amu Å^2, the planar contribution of a hydrogen atom, whereas breaking planarity involves the larger contribution of out-of-plane carbon atoms.[43,44] Albeit small, $3SiCPF_2$ and 3SiCP are both closer in

Table 9 Experimentally determined microwave r_s structure values compared to theoretical r_e and electron diffraction[20] for $3SiCPF_2$

Bond or angle	r_e	$r_s(^{29}Si)$	$r_s(^{30}Si)$	Elec. diff.[20]
$C_1{=}C_2$/Å	1.340	1.3482(79)[a]	1.3482(79)	1.378(7)
$C_2{-}C_3$/Å	1.517	1.5593(97)	1.5593(97)	1.519[b]
Si–C_3/Å	1.869	1.942(30)	1.86(24)	1.847(3)
Si–C_4/Å	1.869	1.729(28)	1.85(24)	1.847(3)
$C_1{-}C_4$/Å	1.517	1.5593(97)	1.5593(97)	1.519[b]
$C_1{-}C_4{-}$Si/°	101.0	102.70(90)	99.8(60)	102.7(4)
$C_3{-}$Si$-C_4$/°	98.8	101.29(53)	100.24(89)	98.7(4)
$C_2{=}C_1{-}C_4$/°	119.6	118.62(65)	118.62(65)	117.9(3)
$C_2{-}C_3{-}$Si/°	101.0	97.35(74)	99.5(59)	102.7(4)
$C_1{=}C_2{-}C_3$/°	119.6	118.62(65)	118.62(65)	117.9(3)
$C_4{-}C_1{=}C_2{-}C_3$/°	0.00	0.0(54)	0.0(54)	—[d]
$C_1{=}C_2{-}C_3{-}$Si[c]/°	0.00	−7.2(40)	−11.6(60)	13.9(8)

[a] Numbers in parentheses represent the 1 s uncertainties (67% confidence interval) from the Costain errors[42] in the least significant figure. [b] Fixed in ref. 20. [c] Reported as δ in ref. 20. [d] Not reported in ref. 20.

Table 10 Second moment comparisons of similar molecules

Molecule	P_{aa}/amu Å^2	P_{bb}/amu Å^2	P_{cc}/amu Å^2
$3SiCPF_2$[a]	217.32825(29)[b]	78.85566(29)	63.72842(29)
$2SiCPF_2$[c]	224.058503(94)	77.698347(94)	62.708151(94)
$SiCPF_2$[d]	227.27110(12)	83.037692(12)	67.164670(12)
3SiCP[a]	105.13543(15)	78.74044(15)	6.22421(15)
SiCP[e]	109.853881(11)	80.028848(11)	12.305876(11)

[a] This work. [b] Numbers in parentheses represent 1 s uncertainties (67% confidence interval) given in units of the least significant figure. [c] Ref. 21. [d] Ref. 44. [e] Ref. 45.

their P_{bb} value to planar $2SiCPF_2$ than nonplanar SiCP and $SiCPF_2$, therefore bringing us to conclude the molecule is planar as the equilibrium structure would suggest.

Curious motions

As discussed in previous subsections, splitting was observed in the spectra of both molecules. This splitting was fit using either one or two Coriolis coupling terms and an energy splitting for the two levels. Furthermore, in $3SiCPF_2$, for which there was previous microwave data, these additions improved the fit of the dataset in the global fit so much that it was concluded that this must be the correct approach to this molecule.

Although significant evidence exists for both molecules containing a motion of some sort, it is unclear as to the source of such a motion. From the calculations we presented earlier, it is obvious that this motion doesn't come from an inversion barrier in the puckering coordinate. Extensively high-level calculations presented here show that each 3SiCP and $3SiCPF_2$ may have very flat wells, but they do not actually increase in energy to form a barrier. Even when calculations are presented that result in a barrier, that barrier is not high enough to adequately represent the level separation determined by our spectroscopic analysis. This makes the source of this splitting very curious, but intriguing and, although we have a large amount of evidence pointing to a motion in 3SiCP and $3SiCPF_2$, we still do not know the source of the motion.

Because our work presented in this manuscript and verified by other previous literature shows that this motion is not due to the puckering coordinate, we will present a couple of hypotheses for the cause here. What we do know is that the Coriolis term F_{bc} is needed indicating a motion about the *a*-axis in the *bc*-plane. The first is a steering wheel wagging motion of the fluorine atoms. Calculations performed by the authors on this motion show there is no discernible barrier that would lead to a splitting of the energy levels. The other, more plausible, source is the shrinkage deformation vibration mentioned in the electron diffraction work in the prior subsection. Being a large amplitude motion, this motion could account for both the observed splitting and the substitution structure differences from the equilibrium structure. However, it isn't clear what is entailed in this motion as there are many possibilities along the ring and, furthermore, what exactly to calculate to begin to test this hypothesis.

Conclusions

The molecules $3SiCPF_2$ and 3SiCP have been synthesized and studied using microwave spectroscopic techniques with accompanying high-level computational approaches. The microwave data collected previously on $3SiCPF_2$ by Durig and Laane[19] has been combined with the new data collected here into a global fit that better describes both sets of experimental transitions. The molecules have both been determined to be planar experimentally using a combination of substitution and planar moment structure approaches. Splitting of spectra observed in both molecules cannot be isolated to a specific source, but the evidence presented here leads the authors to believe that the splitting is not due to an inversion motion from the puckering coordinate. It is speculated that a more comprehensive investigation on all possible large amplitude motions in the molecules needs to be undertaken to determine the source of the motions.

Author contributions

Thomas M. C. McFadden: investigation, formal analysis, writing – original draft, writing – reviewing & editing; Nicole Moon: writing – review & editing, investigation, formal analysis; Frank E. Marshall: investigation, formal analysis; Amanda J. Duerden: investigation, formal analysis; Esther J. Ocola: investigation, formal analysis, writing – original draft, writing – reviewing & editing; Jaan Laane: supervision, formal analysis, writing-reviewing & editing, funding acquisition; Gamil A. Guirgis: supervision, formal analysis, writing – reviewing & editing, funding acquisition; Garry S. Grubbs II: supervision, conceptualization, investigation, formal analysis, writing – original draft, writing – reviewing & editing, funding acquisition.

Conflicts of interest

There are no conflicts to declare.

Acknowledgements

The authors would like to thank Richard Dawes for many helpful conversations and insight. For GSGII, this material is based upon work supported by the National Science Foundation under Grant no. CHE-1841346 and CHE-MRI-2019072. For GAG, the NMR spectrometer at the College of Charleston is supported by the National Science Foundation under grant No. 1429308. JL and EJO wish to thank the Welch Foundation (Grant A-0396) for financial support, and the Texas A&M High Performance Research Computing and the Laboratory for Molecular Simulation at Texas A&M University, College Station for computational resources.

Notes and references

1 J. Laane; E. J. Ocola and H. J. Chun, Vibrational Potential Energy Surfaces in Ground and Excited Electronic States, in *Frontiers and Advances in Molecular Spectroscopy*, ed. J. Laane, Elsevier, Amsterdam, The Netherlands, 2017, pp. 101–142.
2 J. Laane, Vibrational Potential Energy Surfaces in Electronic Excited States, in *Frontiers of Molecular Spectroscopy*, ed. J. Laane, Elsevier, Amsterdam, The Netherlands, 2009, pp. 63–132.
3 J. Laane, Experimental Determination of Vibrational Potential Energy Surfaces and Molecular Structures in Electronic Excited States., *J. Phys. Chem. A*, 2000, **104**, 7715–7733.

4 J. Laane, Vibrational Potential Energy Surfaces of Non-Rigid Molecules in Ground and Excited Electronic States, in *Structures and Conformations of Non-Rigid Molecules*, ed. J. Laane, M. Dakkouri, B. V. D. Veken and H. Oberhammer, Kluwer Publishing, Amsterdam, 1993, pp. 65–98.
5 J. Laane, Spectroscopic Determination of Ground and Excited State Vibrational Potential Energy Surfaces., *Int. Rev. Phys. Chem.*, 1999, **18**, 301–341.
6 J. Laane, Vibrational Potential Energy Surfaces and Conformations of Molecules in Ground and Excited Electronic States., *Annu. Rev. Phys. Chem.*, 1994, **45**, 179–211.
7 J. Laane, Determination of Vibrational Potential Energy Surfaces from Raman and Infrared Spectra., *J. Pure Appl. Chem.*, 1987, **59**, 1307–1326.
8 L. A. Carreira, R. C. Lord and T. B. Mallory, Jr., *Top. Curr. Chem.*, 1979, **82**, 1.
9 J. Laane, One-Dimensional Potential Energy Functions in Vibrational Spectroscopy, *Quart. Rev.*, 1971, **25**, 533–552.
10 R. P. Bell, The Occurrence and Properties of Molecular Vibrations with V, *Proc. R. Soc. London, Ser. A*, 1945, **183**, 328–337.
11 J. Laane and R. C. Lord, Far-Infrared Spectra of Ring Compounds. II. The Spectrum and Ring-Puckering Potential Function of Cyclopentene, *J. Chem. Phys.*, 1967, **47**, 4941–4945.
12 J. Laane, Far-Infrared Spectra and the Ring-Puckering Potential Function of Silacyclopent-3-ene and Silacyclopent-3-ene-1,1-d2, *J. Chem. Phys.*, 1969, **50**, 776–782.
13 J. D. Lewis, T. H. Chao and J. Laane, *J. Chem. Phys.*, 1975, **62**, 1932.
14 T. H. Chao and J. Laane, Vibrational Analyses of Silacyclopent-3-enes, *Spectrochim. Acta*, 1972, **28A**, 2443–2463.
15 R. L. Rosas, C. Cooper and J. Laane, *J. Phys. Chem.*, 1990, **94**, 1830.
16 H. J. Chun, L. F. Colegrove and J. Laane, Theoretical Calculations, Far-Infrared Spectra and the Potential Energy Surfaces of Four Cyclic Silanes., *Chem. Phys.*, 2014, **431-432**, 15–19.
17 P. M. Killough and J. Laane, The Two-Dimensional Potential Energy Surface for the Ring Puckering and Ring Twisting of 1-Silacyclopent-3-ene-d0, 1-d1, and 1,1-d2, *J. Chem. Phys.*, 1984, **80**, 5475–5480.
18 A. Al-Saadi, Further on the molecular structure, vibrational spectra and ring-puckering potentials of silacyclopent-3-ene and its 1,1-dihalo derivatives: Ab initio and DFT study., *Vib. Spectrosc.*, 2012, **62**, 188–199.
19 J. R. Durig, L. A. Carreira and J. Laane, Spectra and Structure of Small Ring Compounds Part XXX*. Microwave Spectrum of 1,1-Difluoro-1-Silacyclopent-3-ene., *J. Mol. Struct.*, 1974, **21**, 281.
20 S. Cradock, E. A. V. Ebsworth, B. M. Hamill, D. W. H. Rankin, J. M. Wilson and R. A. Whiteford, An Electron Diffraction Determination of the Gas-Phase Molecular Structures of 1-Silacyclopent-3-ene, 1,1-Difluoro-1-Silacyclopent-3-ene, and 1,1-Dichloro-1-Silacyclopent-3-ene., *J. Mol. Struct.*, 1979, **57**, 123–133.
21 T. M. C. McFadden, F. E. Marshall, E. J. Ocola, J. Laane, G. A. Guirgis and G. S. Grubbs II, Theoretical Calculations, Microwave Spectroscopy, and Ring-Puckering Vibrations of 1,1-Dihalosilacyclopent-2-enes., *J. Phys. Chem. A*, 2020, **124**(40), 8254.
22 F. E. Marshall, D. J. Gillcrist, T. D. Persinger, S. Jaeger, C. C. Hurley, N. E. Shreve, N. Moon and G. S. Grubbs II, The CP-FTMW Spectrum of Bromoperfluoroacetone., *J. Mol. Spectrosc.*, 2016, **328**, 59–66.
23 F. E. Marshall, R. Dorris, S. A. Peebles, R. A. Peebles and G. S. Grubbs II, The microwave spectra and structure of Ar-1,3-difluorobenzene., *J. Phys. Chem. A*, 2018, **122**, 7385–7390.
24 G. Sedo, F. E. Marshall and G. S. Grubbs, Rotational spectra of the low energy conformers observed in the (1*R*)-(−)-myrtenol monomer., *J. Mol. Spectrosc.*, 2019, **356**, 32–36.
25 F. E. Marshall, J. L. Neill, M. T. Muckle, B. H. Pate, Z. Kisiel and G. S. Grubbs II, Observation of 36ArH35Cl, 38ArH35Cl and 38ArH37Cl in Natural Abundance using CP-FTMW Spectroscopy, *J. Mol. Spectrosc.*, 2018, **344**, 34–38.
26 A. Duerden, F. E. Marshall, N. Moon, C. Swanson, K. M. Donnell and G. S. Grubbs II, A chirped pulse Fourier transform microwae spectrometer with multi-antenna detection, *J. Mol. Spectrosc.*, 2021, **376**, 111396.
27 Z. Kisiel and J. Kosarzewski, *Acta Phys. Pol., A*, 2017, **131**, 311.
28 M. J. Frisch, G. W. Trucks, H. B. Schlegel, G. E. Scuseria, M. A. Robb, J. R. Cheeseman, G. Scalmani, V. Barone, G. A. Petersson, H. Nakatsuji, X. Li, M. Caricato, A. V. Marenich, J. Bloino, B. G. Janesko, R. Gamperts, B. Mennucci, H. P. Hratchian, J. V. Ortiz, A. F. Izmaylov, J. L. Sonnenberg, D. Williams-Young, F. Ding, F. Lipparini, F. Egidi, J. Goings, B. Peng, A. Petrone, T. Henderson, D. Ranasinghe, V. G. Zakrzewski, J. Gao, N. Rega, G. Zheng, W. Liang, M. Hada, M. Ehara, K. Toyota, R. Fukuda, J. Hasegawa, M. Ishida, T. Nakajima, Y. Honda, O. Kitao, H. Nakai, T. Vreven, K. Throssell, J. A. Montgomery Jr., J. E. Peralta, F. Ogliaro, M. J. Bearpark, J. J. Heyd, E. N. Brothers, K. N. Kudin, V. Staroverov, T. A. Keith, R. Kobayashi, J. Normand, K. Raghavachari, A. P. Rendell, J. C. Burant, S. S. Iyengar, J. Tomasi, M. Cossi, J. M. Millam, M. Klene, C. Adamo, R. Cammi, J. W. Ochterski, R. L. Martin, K. Morokuma, Ö. Farkas, J. B. Foresman and D. J. Fox, *Gaussian 16, Revision B.01*, Gaussian, Inc., 340 Quinnipiac Street, Building 40, Wallingford, CT, 2016, p. 06492.
29 R. D. Dennington II, T. A. Keith and J. M. Millam, *GaussView 6.1.1. Semichem*, Inc., Shawnee, KS, 2000–2019.
30 R. W. Schmude, Jr., M. A. Harthcock, M. B. Kelly and J. Laane, Calculation of Kinetic Energy Functions for the Ring-Puckering Vibration of Asymmetric Five-Membered Rings, *J. Mol. Spectrosc.*, 1987, **124**, 369–378.
31 *Maple*, Waterloo Maple, Inc., Waterloo, ON, Canada, 2015.
32 N. Meinander and J. Laane, Computation of the Energy Levels of Large-Amplitude Low-frequency Vibrations. Comparison of the Prediagonalized Harmonic Basis and the Prediagonalized Distributed Gaussian Basis, *J. Mol. Struct.*, 2001, **569**, 1–24.
33 H. M. Pickett, The Fitting and Prediction of Vibration-Rotation Spectra with Spin Interactions., *J. Mol. Spectrosc.*, 1991, **148**, 371–377.

34 Z. Kisiel, L. Pszczolkowski, I. R. Medvedev, M. Winnewisser, F. C. D. Lucia and C. E. Herbst, Rotational spectrum of trans–trans diethyl ether in the ground and three excited vibrational states, *J. Mol. Spectrosc.*, 2005, **233**, 231–243.
35 J. K. G. Watson, *Vibrational Spectra and Structure*, Elsevier, Amsterdam, 1977, vol. 6, p. 1.
36 Z. Kisiel, PROSPE-Programs for ROtational SPEctroscopy, http://info.ifpan.edu.pl/~kisiel/prospe.htm.
37 G. S. Grubbs II, C. T. Dewberry, K. C. Etchison, K. E. Kerr and S. A. Cooke, A Search Accelerated Correct Intensity Fourier Transform Microwave Spectrometer with Pulsed Laser Ablation Source, *Rev. Sci. Instrum.*, 2007, **78**, 096106.
38 H. M. Pickett, Vibration-Rotation Interactions and the Choice of Rotating Axes for Polyatomic Molecules., *J. Chem. Phys.*, 1972, **56**, 1715–1723.
39 J. Kraitchman, Determination of Molecular Structure from Microwave Spectroscopic Data, *Am. J. Phys.*, 1953, **21**, 17–24.
40 J. E. Isert, F. E. Marshall, W. C. Bailey and G. S. Grubbs II, Dipole forbidden, nuclear electric quadrupole allowed transitions and chirality: the broadband microwave spectrum and structure of 2-bromo-1,1,1,2-tetrafluoroethane., *J. Mol. Struct.*, 2020, **1216**, 128277.
41 H. D. Rudolph, Extending Kraitchman's Equations., *J. Mol. Spectrosc.*, 1981, **89**, 430–439.
42 C. C. Costain, *Trans. Am. Crystallogr. Assoc.*, 1966, **2**, 157.
43 R. K. Bohn, J. A. Montgomery, H. H. Michels and J. A. Fournier, Second moments and rotational spectroscopy, *J. Mol. Spectrosc.*, 2016, **325**, 42–49.
44 N. Moon, F. Marshall, T. McFadden, E. Ocola, J. Laane, G. Guirgis and G. S. Grubbs II, Pure rotational spectrum and structure determination of 1,1-difluoro-1-silacyclopentane, *J. Mol. Struct.*, 2022, **1249**, 131563.
45 Z. Chen and J. van Wijngaarden, Pure rotational spectrum and structural determination of silacyclopentane., *J. Mol. Spectrosc.*, 2011, **269**, 137–140.

